

Forward Behavioral Modeling of Concurrent Dual-Band Power Amplifiers Using Extended Real Valued Time Delay Neural Networks

Zihong Huang¹, Wenhua Chen¹, Zhenghe Feng¹, Fadhel M. Ghannouchi²

¹Department of Electronic Engineering, Tsinghua University, China, 10084

²Radio Lab., Department of Electrical and Computer Engineering, University of Calgary, Canada

Abstract- The distortions induced by inter-modulations and cross-modulations in concurrent dual-band power amplifiers (PAs) are evidenced and characterized using multi-tone signals. Given the presence of cross-modulations, a comprehensive extended real-valued time-delay neural network (extended-RVTDNN) is proposed to model the nonlinear behavior of concurrent dual-band PAs. Two three-carrier WCDMA signals are applied to a dual-band Doherty PA prototype for modeling verification. The experimental results show that the proposed model approximates the PA with normalized mean square errors (NMSEs) of -38.48dB and -35.42dB in the lower and upper bands, respectively. Compared with the conventional single-band RVTDNN, this new method achieves an improvement in accuracy of more than 10dB.

Key words- Power amplifiers, memory effects, cross modulation, neural networks

I. INTRODUCTION

With the rapid expansion of modern high-speed wireless communications, mobile communication systems should accommodate many standards simultaneously, especially for the upcoming long-term evolution advanced (LTE-Advanced) system. Corresponding to this trend, radio frequency (RF) components are often required to operate in multiple modes and support compatibility across different systems [1]. To satisfy this requirement, multiband power amplifiers (PAs) will be highly desirable in future wireless communication systems. Many studies on the design of concurrent dual-band PAs have been published recently.

The digital pre-distortion (DPD) technique is a widely accepted linearization approach that provides high accuracy in synthesizing the pre-distortion function and leads to a higher efficiency by allowing PAs to operate near saturation. DPD relies on the introduction of an exact inverse nonlinear pre-distorter before the PA to compensate for nonlinearity.

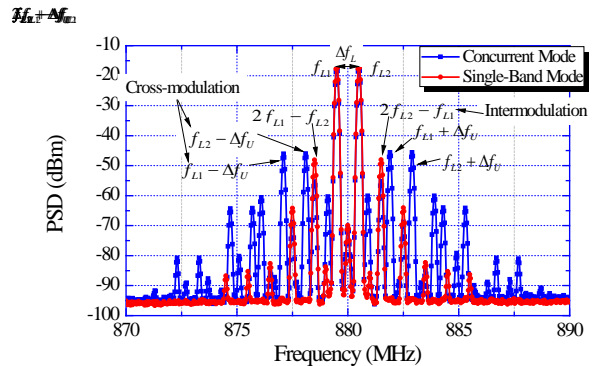
Many nonlinear models have been proposed for the characterization of PAs, including the memory polynomial model, the Volterra model, Wiener and Hammerstein models, and neural networks (NNs) models. In particular, NN models, with their excellent approximation capability, are becoming an increasingly attractive solution for PA behavioral modeling. NN models have been mostly used to successfully model single-band PAs [2]. To the best of our knowledge, there is no precedent NN model that has been applied for the behavioral modeling in concurrent dual-band PAs.

On account of the distortion caused by cross-modulations, an extended real-valued time-delay NN (RVTDNN) model is proposed to approximate the nonlinear behavior of concurrent dual-band PAs. The proposed model is trained and validated with different segments of the overall test data, and the experimental results demonstrate the advantage of this method.

II. NONLINEARITY CHARACTERIZATION OF CONCURRENT DUAL-BAND PAs

As first shown in [3], in the modeling of the concurrent dual-band PA with a simple fifth-order memory-less nonlinear model, the output signals around the carrier frequencies in the dual bands can be derived. In [3], both input signals contribute to the nonlinearities of the output signals in dual bands are indicated. For these terms to be evidenced and the nonlinear behavior of concurrent dual-band PAs to be identified, two 2-tone signals are used for characterization [4]. As shown in Fig.1, each band has a symmetrical 2-tone signal around its central frequency; and the frequency spacing in the lower and upper bands are set to 1 MHz and 2.4 MHz, respectively.

The measured output spectra of a dual-band PA prototype [5] in concurrent and single-band modes are compared in Fig.1. It is not difficult to determine that many new modulation products occur in the spectrum of concurrent mode, which do not exist in the single-band mode. According to (1) and (2), we can figure out that these new terms are induced by the cross-modulation of the signals in different bands. The produced inter-modulations and cross-modulations are as labeled in Fig.1. For simplicity, only productions up to the third order are marked.



(a)

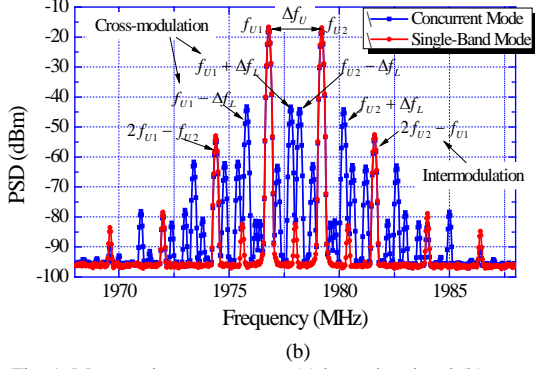


Fig. 1. Measured output spectra: (a) lower band and (b) upper band

For the purpose of wideband and dynamic behavioral modeling, memory effects cannot be neglected. Following the definition in [6], the intensity of memory effects is quantified by the difference between the modulation products on both sides of the carrier frequency. We define the memory effect metrics as the imbalance between the right and left modulation products. In frequency sweeping scheme, the inter-modulation and cross-modulation products do not overlap in the output spectrum and the cross-modulations experience significant memory effects, especially the far cross-modulations. This effect is attributed to the expansion of the frequency spacing, since the memory effects of PAs are associated with the bandwidth of the input signal [6].

III. EXTENDED-RVTDNN FOR DUAL-BAND PA

A comprehensive survey on different NN models for PA modeling can be found in [2]. In this paper, a brief review is presented. First, a single-input, single-output, feed-forward NN uses complex input and output signals, which results in high calculation complexity. Uncoupled NNs that model output amplitude and phase (or I and Q components) separately are limited by asynchronous convergence. The real-valued feed-forward neural network (RVFFNN) model, which takes advantage of the I and Q components in the baseband signals, reduces the complexity of a neural network. However, with the continuously growing modulation bandwidth of signals, no paper has yet considered the memory effects with RVFFNN. A real-valued time-delay neural network (RVTDNN), based on a feed-forward neural network (FFNN), has been well established for wideband PA modeling. It models memory effects successfully by importing tapped delay lines (TDLs) in the baseband inputs [2].

Concurrent dual-band PAs exhibit more complex behavior than that of single-band PAs; and, the distortions caused by cross-modulations should be taken into account. Certainly, the memory effects of all products should also be included. To meet this requirement, an extended real-valued time-delay neural network (extended-RVTDNN) is proposed to approximate the nonlinear behavior of concurrent dual-band PAs, the topology of which is illustrated in Fig.2. To fully consider the cross-modulations, two single-band RVTDNNs are combined with mutual coupling; thus, the conventional

model is extended to a new neural network with four inputs and four outputs. Due to the coupling of two single-band NNs, the cross-modulation products of the two input signals in (1) and (2) can be automatically integrated into the NN. As highlighted in the shadowed area of Fig.2, the conventional single-band RVTDNN can be regarded as a special case, with the remaining network idle.

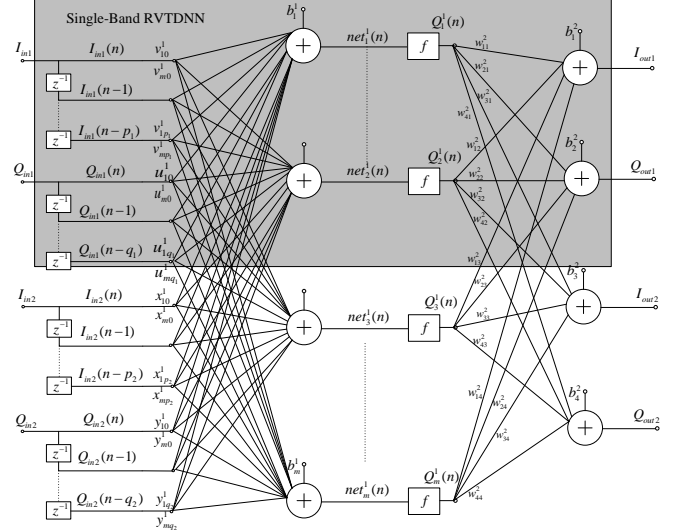


Fig. 2. Block diagram of extended-RVTDNN for dual-band PA behavioral modeling

Since the inter-modulation and cross-modulation products both contribute to the nonlinearity of the PA, the outputs in dual bands are all functions of the two input signals:

$$I_{out1}(n) = g_1 [I_{in1}(n), I_{in1}(n-1), \dots, I_{in1}(n-p_1); Q_{in1}(n), Q_{in1}(n-1), \dots, Q_{in1}(n-q_1); \quad (1)$$

$$I_{in2}(n), I_{in2}(n-1), \dots, I_{in2}(n-p_2); Q_{in2}(n), Q_{in2}(n-1), \dots, Q_{in2}(n-q_2)] \quad (1)$$

$$Q_{out1}(n) = g_2 [I_{in1}(n), I_{in1}(n-1), \dots, I_{in1}(n-p_1); Q_{in1}(n), Q_{in1}(n-1), \dots, Q_{in1}(n-q_1); \quad (2)$$

$$I_{in2}(n), I_{in2}(n-1), \dots, I_{in2}(n-p_2); Q_{in2}(n), Q_{in2}(n-1), \dots, Q_{in2}(n-q_2)] \quad (2)$$

$$I_{out2}(n) = g_3 [I_{in1}(n), I_{in1}(n-1), \dots, I_{in1}(n-p_1); Q_{in1}(n), Q_{in1}(n-1), \dots, Q_{in1}(n-q_1); \quad (3)$$

$$I_{in2}(n), I_{in2}(n-1), \dots, I_{in2}(n-p_2); Q_{in2}(n), Q_{in2}(n-1), \dots, Q_{in2}(n-q_2)] \quad (3)$$

$$Q_{out2}(n) = g_4 [I_{in1}(n), I_{in1}(n-1), \dots, I_{in1}(n-p_1); Q_{in1}(n), Q_{in1}(n-1), \dots, Q_{in1}(n-q_1); \quad (4)$$

$$I_{in2}(n), I_{in2}(n-1), \dots, I_{in2}(n-p_2); Q_{in2}(n), Q_{in2}(n-1), \dots, Q_{in2}(n-q_2)] \quad (4)$$

where p_1 , q_1 , p_2 and q_2 are the memory depths of the input vectors, and functions g_i are modeled by the proposed extended-RVTDNN.

Apparently, the output signal in each band is not only the response of the input signal at its own frequency, but also the contribution of the two signals in dual bands. The delayed response is achieved by using the delay operator. The TDLs store values from the previous time step, which can be used in the current step. The outputs can be expressed as:

$$I_{out(i+1)} = \sum_{k=1}^m w_{(2i+1)k}^2 Q_k^1(n) + b_{(2i+1)}^2, \quad i = 0, 1 \quad (5)$$

$$Q_{out(i+1)} = \sum_{k=1}^m w_{(2i+2)k}^2 Q_k^1(n) + b_{(2i+2)}^2, \quad i = 0, 1 \quad (6)$$

$$\text{Where, } Q_k^1(n) = f(\text{net}_k^1(n)) \quad k = 1, 2, \dots, m \quad (7)$$

$$\begin{aligned}
net_k^1(n) &= \sum_{i=0}^{p_1} v_{ki}^1 I_{in1}(n-i) + \sum_{i=0}^{q_1} u_{ki}^1 Q_{in1}(n-i) \\
&+ \sum_{i=0}^{p_2} x_{ki}^1 I_{in2}(n-i) + \sum_{i=0}^{q_2} y_{ki}^1 Q_{in2}(n-i) + b_k^1
\end{aligned} \quad (8)$$

The chosen activation function for the hidden layer is the tansig function given as:

$$f(x) = \tanh(x) = \frac{1 - e^{-2x}}{1 + e^{2x}} \quad (9)$$

To implement this NN model, the synaptic weights in (7)-(10) have to be extracted based on tested data. In order to guarantee high modeling accuracy and low computation complexity, the training algorithm for the NN needs to be selected carefully. In [2], different training algorithms for NNs were compared in terms of accuracy and speed, and the Levenberg-Marquart (LM) algorithm [7] outperformed the others, due to its fast convergence and good accuracy. As a result, the LM algorithm is chosen for NN training in this study.

IV. EXPERIMENTAL RESULTS

The details of the applied concurrent dual-band PA prototype for validation can be found in [5].

Fig.3 presents a test bed united by two identical and phase coherent vector signal generators (ESG 4438C) with an external oscillator, spectrum analyzer (E4440A), 89600 vector signal analysis software and MATLAB. The third signal generator is used as an external oscillator to synchronize the two signal generators, which can guarantee high synchronization accuracy. The dual-band PA is excited with a WCDMA101 signal (a three-carrier WCDMA signal with the center carrier turned off) in the lower band and a WCDMA111 signal (a three-carrier wideband code division multiple access signal with all three carriers present) in the upper band, respectively.

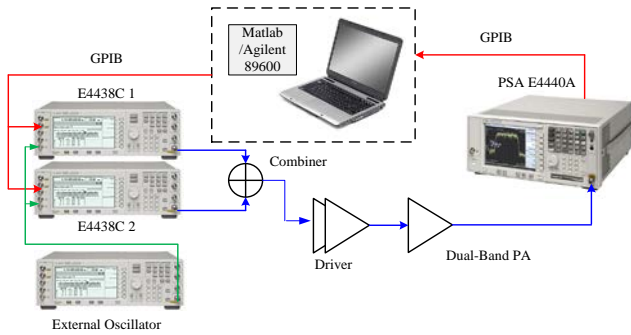


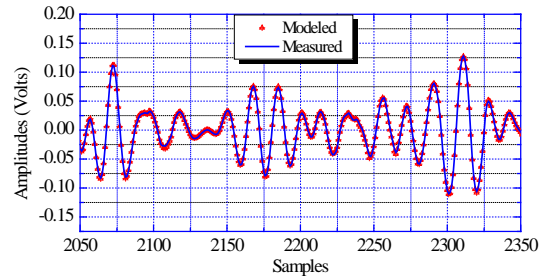
Fig. 3. Test bed for behavioral modeling

The two signal generators act as synthesizers and up-converters of the baseband signals to their respective RF frequencies, where they are combined together using a Wilkinson power combiner. The combined signal drives a wideband pre-amplifier PA (AR 5S1G4) cascaded with a concurrent dual-band Doherty PA. Finally, the output signal is

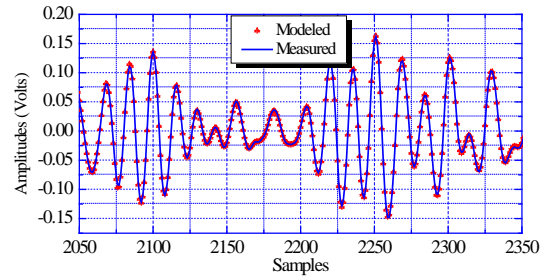
captured by the Agilent PSA E4440A spectrum analyzer and vector signal analyzer (VSA89000). The PAPR of the two signals before pre-distortion is around 10.5 dB, their chip rate is 3.84 Mc/s, and the peak output powers in dual bands are both kept at 37 dBm, which operates near saturation. The PA is operated at 880 MHz and 1978 MHz for the measurements.

The model training and validation is implemented in a MATLAB environment. Two different segments with 4000 data points in each band are selected from the overall collected test data and used for training and validation. The selected segments should contain the fast transition states of the waveform as much as possible, in order to improve the modeling accuracy. After careful comparative studies, it was determined that a single hidden layer is sufficient for the modeling; and, the extended-RVTDNN model uses 30 neurons in the single hidden layer and 3 taps in four input TDLs.

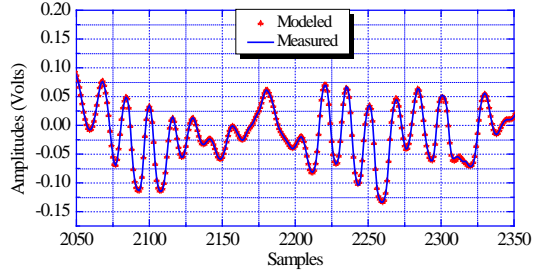
Fig.4 shows the validated results of the I and Q components in the time domain. The predicted and measured results agree well in all four components. It demonstrates that the extended-RVTDNN model for concurrent dual-band PA accurately approximates the PA. A comparison of the output spectra of the single-band RVTDNNs without mutual coupling, the extended-RVTDNN and the real measurement results is illustrated in Fig.5. It can be seen that the proposed extended-RVTDNN achieves higher accuracy than the single-band RVTDNN, due to the integration of the additional distortions induced by the cross-modulations.



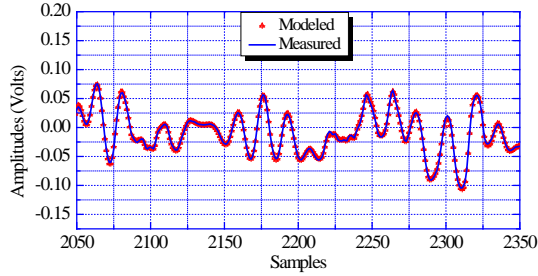
(a) I component in lower band



(b) Q component in lower band

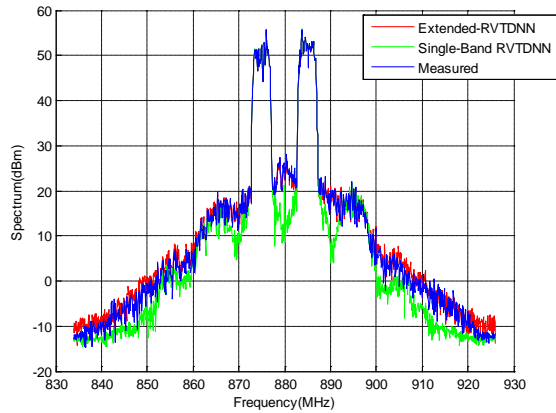


(c) I component in upper band

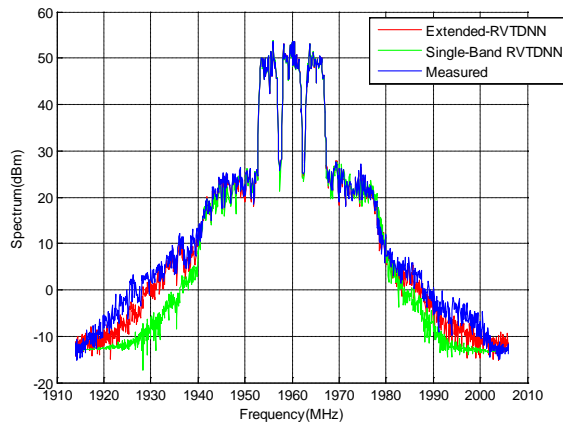


(d) Q component in upper band

Fig. 4. Validation results of I and Q components



(a) Lower ban



(b) Upper band

Fig. 5. Comparison of output spectrum between the single-band RVTDNN, extended-RVTDNN and the measured data of three-carrier WCDMA signals.

To evaluate the accuracy of the proposed model, the normalized mean square errors (NMSE) for each band is

summarized in Table I, which shows that the extended-RVTDNN achieves an improvement in modeling accuracy of more than 10dB.

TABLE I.
SUMMARY OF NMSE

Frequency (MHz)	Signal	NMSE (dB)	
		Single-Band RVTDNN	Extended-RVTDNN
880	WCDMA101	-27.90	-38.48
1978	WCDMA111	-21.91	-35.42

V. CONCLUSION

In this paper, the distortions induced by inter-modulations and cross-modulations in concurrent dual-band PAs are both taken into consideration. To model the behavior of the concurrent dual-band PA, an extended real-valued time-delay neural network (RVTDNN) is proposed to predict the nonlinearity and memory effects of the concurrent dual-band PA. The dual-band PA is driven with three-carrier WCDMA signals, and good agreement is shown between the extended-RVTDNN model output and the measurement results in the time and frequency domains. The proposed model achieves NMSEs of -38.48dB and -35.42dB for the lower and upper bands, respectively. Compared with the conventional single-band RVTDNN, the proposed method achieves an improvement in modeling accuracy of more than 10dB.

ACKNOWLEDGMENT

This work was supported by the National Science and Technology Major Project of the Ministry of Science and Technology of China under Grant No. 2010ZX03007-003 and 2012ZX03001009-003, Agilent Technologies Foundation (2414-CN11).

REFERENCES

- [1] R.-C. Hua, C.-F. Chou, S.-J. Wu, T.-G. Ma, "Compact multiband planar monopole antennas for smart phone applications," *IET Microwaves, Antennas & Propagation*, Vol. 2, No. 5, May 2008, pp. 473–481.
- [2] M. Rawat, K. Rawat, Fadhel M. Ghannouchi, "Adaptive Digital Predistortion of Wireless Power Amplifiers/Transmitters Using Dynamic Real-Valued Focused Time-Delay Line Neural Networks," *IEEE Transactions on Microwave Theory and Techniques*, Vol. 58, No. 1, Jan. 2010, pp. 95–104.
- [3] Seyed Aidin Bassm, "Advanced Signal Processing Techniques for Impairments Compensation and Linearization of SISO and MIMO Transmitters," *Doctor Dissertation*, University of Calgary, Sep. 2010.
- [4] David H. Wisell, Bjorn Rudlund, Daniel Ronnow, "Characterization of memory effects in power amplifiers using digital two-tone measurements," *IEEE Transactions on Instrument and Measurement*, Vol. 56, No. 6, Dec. 2007, pp. 2757–2766.
- [5] Xiang Li, Wenhua Chen, Zhijun Zhang, Zhengfe Feng, Xinyi Tang, Koen Mouthaan, "A Concurrent Dual-Band Doherty Power Amplifier," *Asia-Pacific Microwave Conference*, Yokohama, Japan, Dec. 2010, pp. 654–657.
- [6] Hyunchul Ku, Michael D. McKinley, J. Stevenson Kenny, "Quantifying memory effects in RF power amplifiers," *IEEE Transactions on Microwave Theory and Techniques*, Vol. 50, No. 12, Dec. 2001, pp. 2843–2849.
- [7] R. Battiti, "First- and Second-Order Methods for Learning: Between Steepest Descent and Newton's Method," *Neural Computation*, Vol. 4, No. 2, Mar. 1992, pp. 141–166.